Available online at www.sciencedirect.com
SCIENCE DIRECT®
Applied Catalysis A: General 247 (2003) 143–156
APPLIED CATALYSIS A: GENERAL
www.elsevier.com/locate/apcata

Skeletal isomerization of linear butenes on tungsten promoted ferrierite

Zunilda R. Finelli, Carlos A. Querini, Raúl A. Comelli*

Instituto de Investigaciones en Catálisis y Petroquímica (INCAPE) (FIQ-UNL, CONICET), Santiago del Estero 2654, S3000AO J-Santa Fe, Argentina

Received 13 September 2002; received in revised form 16 January 2003; accepted 18 January 2003

Abstract

Samples of ammonium, protonic and potassium ferrierites were impregnated with tungsten species. The catalytic behavior of samples with and without tungsten during the linear butene isomerization reaction was studied. Tungsten loadings between 0.5 and 1.0% on ammonium ferrierite produce a synergetic effect both on activity and isobutene yield, while tungsten addition on the protonic form worsens the catalytic behavior of the unpromoted ferrierite. The presence of tungsten species on potassium ferrierite promotes the linear butene skeletal isomerization, with an optimum in the performance when the tungsten loading is between 3.5 and 4.0%. Tungsten species show a weak interaction with the potassium ferrierite surface. On the other hand, on protonic ferrierite the interaction is slightly stronger than on ammonium ferrierite, and the reduction of tungsten occurs practically in one step. The effect of both pretreatment and operational conditions over catalytic performance and deactivation of materials was also addressed. The higher the calcination temperature of ammonium ferrierite, the lower the linear butene conversion and the isobutene yield. Protonic ferrierite, tungsten promoted ammonium ferrierite, and tungsten promoted protonic ferrierite show similar qualitatively behaviors. After 5 min of reaction at any operational conditions, a high activity with low isobutene selectivity is observed. This behavior is related to the presence of strong acid sites. At long time-on-stream (TOS), the linear butene conversion at 450 °C is significantly higher than the one reached at 300 °C, while the isobutene yield remains between 12 and 18% for both reaction temperatures. Tungsten promoted potassium ferrierite samples display a different behavior. At 5 min the high activity is not reached, and both linear butene conversion and isobutene yield appear more stable with TOS; what is associated with the absence of strong acid sites. When reaction takes place at 450 °C, the isobutene yield significantly increases, approaching the yield obtained with the other samples. For all samples, the presence of hydrogen previously and during the reaction does not significantly modify the catalytic behavior, showing a small effect over the by-product distribution. By-products are formed from oligomers, which are among the products even at long TOS.

The level of the carbonaceous deposit formed during reaction on protonic ferrierite, tungsten promoted ammonium ferrierite, and tungsten promoted protonic ferrierite was usually 6.0–7.8 wt.%. The oxidation profiles displayed two combustion peaks when the reaction took place at 300 °C, and only a high-temperature combustion peak when the reaction was carried out at 450 °C. On tungsten promoted potassium ferrierite, the deposit was considerably smaller (0.3–0.7 wt.%); coke formed at 300 °C showed a well-defined combustion peak at moderate temperature, while only a high-temperature combustion peak

* Corresponding author. Tel.: +54-342-4528062; fax: +54-342-4531068.
E-mail address: rcomelli@fiqus.unl.edu.ar (R.A. Comelli).

0926-860X/03/$ – see front matter
doi:10.1016/S0926-860X(03)00094-2

appeared when the deposit was formed at 450 °C. The amount of carbonaceous deposit is associated to the strength of acid sites while its nature is more strongly influenced by the reaction temperature.

Keywords: Tungsten–ferrierite; Skeletal isomerization; Isobutene; Tungsten loading; Pretreatment; Deactivation

1. Introduction

In the last few years, the skeletal isomerization of linear butenes has achieved an increasing practical interest as an alternative route for the production of isobutene, which is used for the methyl *tert*-butyl ether synthesis and in alkylation reactions. The isomerization reaction takes place on acid catalysts. Ferrierite is a zeolite with a bidimensional pore structure of 10-membered rings (42 nm × 54 nm) intersected by 8-membered rings (35 nm × 48 nm); it shows one of the best catalytic behaviors [1]. The bidimensional pore structure of ferrierite was considered responsible for the high isobutene selectivity of the material, although it is reached after some time-on-stream (TOS) when a carbonaceous deposit is formed and suppresses undesirable side reactions [2]. The acid strength distribution of ferrierite shows two types of acid sites, having weak and strong acid strength, respectively [1–3]. The high activity at short TOS was related to the strong acid sites [4]. The external acid sites are non-shape selective for isomerization and they are responsible for the side reactions, while the internal acid sites are selective for the skeletal isomerization [5]. Both catalytic activity and isobutene selectivity have also been related to the density of acid sites [6] and to the space around them [7].

The deactivation of acid catalysts, particularly ferrierite, during the linear butene skeletal isomerization has aroused considerable interest. The spatial constraint inside the pores due to the carbonaceous deposit formation has been considered in order to explain the isobutene selectivity enhancement with TOS. An exhaustive analysis of the deactivation of solid acid catalysts during the butene skeletal isomerization, considering the beneficial and harmful effects of carbonaceous deposits, has recently been reported [8].

Previous results [9] have shown that potassium ferrierite is inactive for the linear butene skeletal isomerization, while tungsten species on this material promote the isobutene formation. Protonic ferrierite presents a high linear butene conversion and the addition of tungsten species on ammonium ferrierite generates a synergetic effect over the isobutene production. The carbonaceous deposit formed during this reaction was also characterized [3].

The influence of operational conditions, such as temperature, 1-butene partial pressure, and weight hourly space velocity over the catalytic performance of ferrierite during the linear butene skeletal isomerization has also been reported [10,11]. In order to improve the catalytic behavior of tungsten promoted ferrierite catalysts in this reaction, the optimal tungsten loadings and both pretreatment and reaction conditions must be determined. Furthermore, no data referred to the effect of the presence of hydrogen over the performance of these materials are available.

In this paper, the catalytic behavior of different ferrierite forms with and without tungsten during the linear butene skeletal isomerization, is studied. Ammonium, protonic and potassium ferrierites were impregnated with tungsten species, being characterized by temperature-programmed reduction (TPR). The optimal tungsten loading on each material is determined. The effect of pretreatment and operational conditions over catalytic performance and deactivation, characterized by temperature-programmed oxidation (TPO), is also analyzed.

2. Experimental

Potassium and ammonium ferrierites, identified as K-FER and NH_4-FER, respectively, were provided by TOSOH, Japan (samples HSZ-720KOA and HSZ-720NHA, respectively). The chemical composition of K-FER and NH_4-FER was $Na_{0.82}K_{2.57}[Al_{3.36}Si_{30.00}O_{66.74}]\cdot nH_2O$ and $Na_{0.03}K_{0.04}[Al_{3.35}Si_{30.00}O_{65.06}]\cdot nH_2O$, respectively. The SiO_2/Al_2O_3 molar ratio was 17.8. The crystalline structure was characterized by X-ray diffraction using a Rich-Seifert Iso-Debyeflex

2002 diffractometer, the diffraction spectrum range being $0 < 2\theta < 60^{\circ}$.

K-FER, NH_4-FER and H-FER (ferrierite in the protonic form obtained by calcining NH_4-FER at 550 °C) samples were impregnated with different tungsten loadings, following the incipient wetness technique and using tungstic acid as the tungsten precursor. Solutions with the calculated concentrations to obtain a given tungsten loading on the solids were prepared. After impregnation, the samples were maintained for 4 h at room temperature, and then dried overnight in an oven at 110 °C. Samples were identified as W(*l*)/K-FER, W(*l*)/NH_4-FER, and W(*l*)/H-FER, *l* being the tungsten loading on the solid, expressed as weight percent referred to the dried base. Tungsten loadings were 2.5–3.0–3.5–4.0% on K-FER and 0.5–1.0–1.5–2.0% on NH_4-FER and H-FER, respectively.

The surface species reducibility was determined by TPR using an Ohkura TP 2002S equipped with a thermal conductivity detector. Samples were pretreated in situ in a nitrogen (60 ml min^{-1}) plus air (50 ml min^{-1}) stream, heating at 9.6 °C min^{-1} and holding 60 min at 600 °C. Then, samples were cooled to room temperature in an argon stream, and finally heated at 10 °C min^{-1} up to 950 °C in a 1.8% hydrogen in argon stream.

The catalytic behavior during the 1-butene skeletal isomerization was measured in a continuous flow fixed-bed quartz tubular reactor operated at atmospheric pressure, using 500 mg of catalyst sieved to 35–80 mesh. Samples were pretreated in situ under different conditions, and then cooled to the desired temperature. For reaction, a pure 1-butene stream was co-fed with either nitrogen or nitrogen plus hydrogen. Different experiments made were the following.

- Reaction at 300 °C on NH_4-FER, H-FER and K-FER with different tungsten loadings.
- Reaction at 300 °C on NH_4-FER calcined at 550, 600, 650 and 700 °C.
- Reaction at 300 and 450 °C on NH_4-FER, H-FER and K-FER with and without tungsten.
- Reaction at 300 °C on NH_4-FER, H-FER and K-FER with and without tungsten, in the absence of hydrogen, feeding hydrogen during pretreatment, and feeding hydrogen during both pretreatment and reaction.

The reactant and reaction products were analyzed by on-line gas chromatography, using a 30 m long, 0.54 mm o.d. GS-Alumina (J&W) megabore column, operated as follows: 5 min at 100 °C, heating at 10 °C min^{-1} up to 160 °C, keeping this temperature for 30 min. From these data, catalytic activity, selectivity to isobutene, isobutene yield, and by-product distribution were calculated on a carbon basis. The catalytic activity is expressed as linear butene conversion, grouping together the three linear butene isomers. It is based on the fact that, under reaction conditions, the 1- to 2-butene isomerization quickly reaches the equilibrium via double-bond migration.

The TPO analysis of used catalysts was performed in an apparatus designed to improve both sensitivity and resolution [12]. Combustion products were completely converted to methane on a nickel catalyst, methane being continuously analyzed by a flame ionization detector. Experiments were carried out using a 6% oxygen in nitrogen stream (20 ml min^{-1}), heating at 12 °C min^{-1}. The sample weight was about 0.01 g. Calibration was periodically checked to verify the total conversion of both carbon monoxide and carbon dioxide into methane.

3. Results

3.1. Optimal tungsten loading on NH_4-FER, H-FER and K-FER

Table 1 shows both catalytic activity, expressed as linear butene conversion, and isobutene yield for NH_4-FER, H-FER, and K-FER impregnated with different tungsten loadings. After 5 min of reaction, H-FER, W/NH_4-FER and W/H-FER present similar linear butene conversions (between 85.9 and 89.8%), W/NH_4-FER reaching the highest isobutene yields. At long TOS, tungsten loadings between 0.5 and 1.0% on NH_4-FER improve the performance of the unpromoted material, while loadings larger than 1.5% unfavor both conversion and isobutene yield under the mild reaction conditions. In the W/H-FER series, the catalyst containing 0.5% tungsten reaches the best catalytic performance, but it is lower than the H-FER corresponding one. W/K-FER samples display a higher stability, keeping catalytic performance with TOS. Loadings between 3.5 and 4.0%

Table 1
Linear butene conversion (X_n-butene) and isobutene yield (Y_i-butene) for NH_4-FER, H-FER and K-FER impregnated with different tungsten loadings, at two TOS

Sample	X_n-butene (%)		Y_i-butene (%)		*i*-butene/*n*-butene[a]	
	5 min	120 min	5 min	120 min	5 min	120 min
H-FER	87.2	20.5	87.2	20.5	1.21	0.17
W(0.5)/NH_4-FER	88.9	24.5	88.9	24.5	1.41	0.21
W(1.0)/NH_4-FER	88.7	22.5	88.7	22.5	1.33	0.18
W(1.5)/NH_4-FER	88.6	10.1	88.6	10.1	1.45	0.08
W(2.0)/NH_4-FER	85.9	13.3	85.9	13.3	1.37	0.10
W(0.5)/H-FER	89.8	12.8	89.8	12.8	1.31	0.10
W(1.0)/H-FER	88.8	11.5	88.8	11.5	1.14	0.08
W(1.5)/H-FER	88.6	7.1	88.6	7.1	0.97	0.06
W(2.0)/H-FER	86.6	8.5	86.6	8.5	0.90	0.06
W(2.5)/K-FER	1.6	1.2	1.6	1.2	0.01	0.01
W(3.0)/K-FER	1.8	1.4	1.8	1.4	0.01	0.01
W(3.5)/K-FER	4.2	3.2	4.2	3.2	0.02	0.01
W(4.0)/K-FER	5.6	3.5	5.6	3.5	0.02	0.01

Reaction at 300 °C, atmospheric pressure and 0.18 atm 1-butene partial pressure.
[a] Thermodynamic equilibrium ratio = 1.35 [27] to 1.41 [28].

allow us to obtain the best behavior, even though the activity is much lower than in the other cases. Considering all data, only the W/NH_4-FER samples at 5 min reach the isobutene/linear butenes thermodynamic equilibrium ratio. The other samples show a lower ratio, being it one order lower for long TOS.

The TPR characterization shows differences according to the impregnated ferrierite form, increasing the intensity of reduction peaks as a function of the tungsten loading. Fig. 1 displays TPR profiles of characteristic samples. The TPR profile of W/NH_4-FER present two-overlapped reduction peaks with maxima at about 775 and 850 °C, respectively. In the case of the W/H-FER profile, a broad reduction peak beginning at 800 °C and with a maximum at about 890 °C is observed. The largest tungsten loading on K-FER produces larger peaks, the main one with a maximum at about 820 °C and the smaller one with a maximum at about 620 °C, where the main envelope begins.

3.2. Effect of calcination temperature

Fig. 2 presents linear butene conversion, isobutene selectivity, and isobutene yield for NH_4-FER calcined between 550 and 700 °C. For each calcination temperature, the catalytic behavior is similar, diminishing activity and improving isobutene selectivity with TOS. This behavior was reported as characteristic for ferrierite [13]. For all temperatures, conversion is practically the same after 5 min of reaction, while at long TOS conversion decreases by increasing the calcination temperature. Independent of TOS, the higher the calcination temperature, the lower the isobutene yield. The isobutene selectivity is the same for any calcination temperature.

3.3. Effect of reaction temperature

Fig. 3 shows the catalytic behavior of samples with and without tungsten when the reaction takes place at 300 and 450 °C. H-FER, W/NH_4-FER and W/H-FER at 5 min and independently of temperature reach a high conversion. At 300 °C, the behavior with TOS is the characteristic one of ferrierite. At 450 °C and long TOS, the activity is higher than the 300 °C corresponding one, and the isobutene selectivity is low without significant differences between the samples. The isobutene yield remains between 12 and 18% for practically all samples. For W/K-FER, both conversion and isobutene yield are low keeping them with TOS when

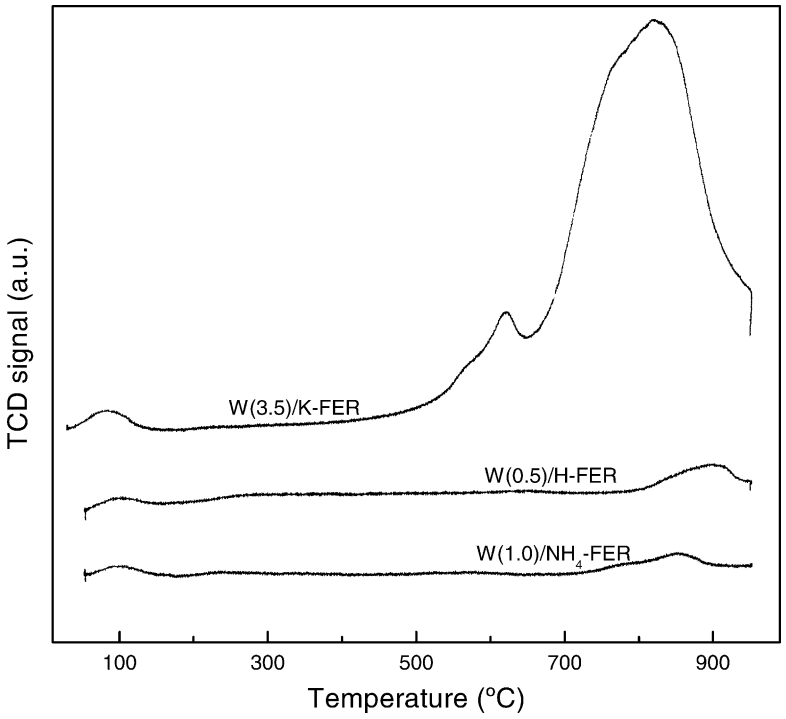

Fig. 1. TPR profiles of characteristic tungsten impregnated samples.

the reaction takes place at 300 °C. At 450 °C the linear butene conversion reaches 40% at 5 min, then slightly decreasing with TOS; the isobutene yield significantly improves, reaching 12%.

3.4. Effect of hydrogen

Fig. 4 allows us to compare the catalytic behavior at 300 °C in the absence of hydrogen, when hydrogen

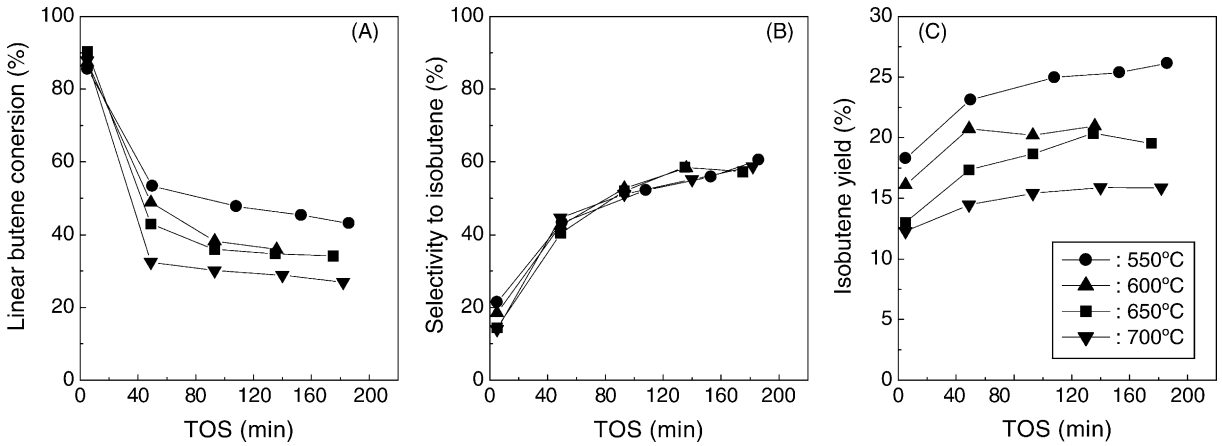

Fig. 2. (A) Linear butene conversion; (B) selectivity to isobutene; and (C) isobutene yield during the 1-butene skeletal isomerization on NH_4-FER calcined at temperatures between 550 and 700 °C. Reaction at 300 °C, atmospheric pressure, and 0.13 atm 1-butene partial pressure.

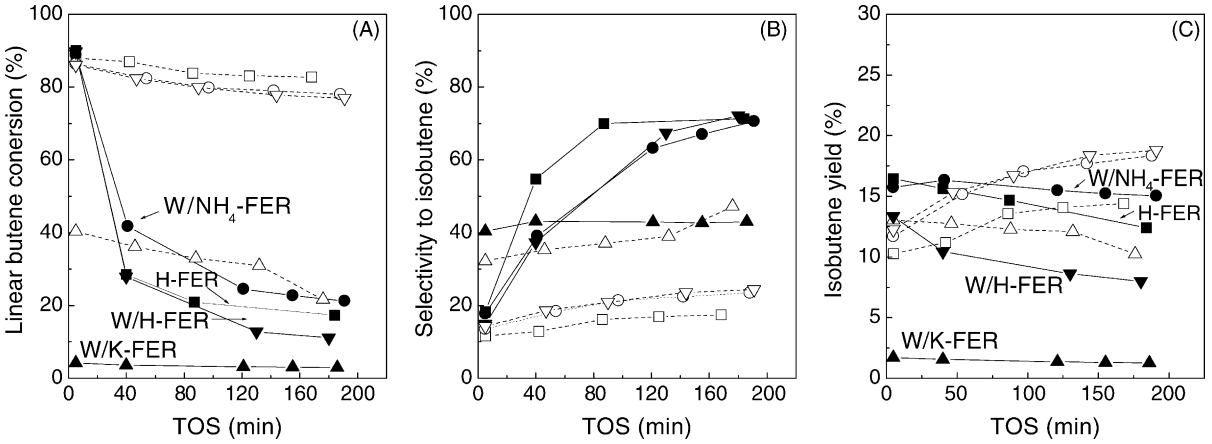

Fig. 3. (A) Linear butene conversion; (B) selectivity to isobutene; and (C) isobutene yield during the 1-butene skeletal isomerization on samples with and without tungsten. Reaction either at 300 °C (filled symbol and solid line) or at 450 °C (open symbol and dashed line), atmospheric pressure, and 0.18 atm 1-butene partial pressure.

is present during pretreatment and when hydrogen is present in pretreatment plus reaction. H-FER, W/NH_4-FER and W/H-FER, with or without the presence of hydrogen, reach a similar high conversion after 5 min. At long TOS, each material presents its characteristic behavior, without significant differences in the catalytic activity due to the presence of hydrogen either during the pretreatment or during the pretreatment and the reaction. Nevertheless, the hydrogen modifies the selectivity and the isobutene yield in different amounts depending on the catalyst. For W/K-FER, the catalytic behavior is practically constant with TOS with a conversion below 10%.

Fig. 5 shows by-product distributions at 300 °C for samples with and without tungsten. The operational conditions are the same as those shown in Fig. 4. For practically all samples and operational conditions, a low proportion of C_1, C_2, and isobutane is

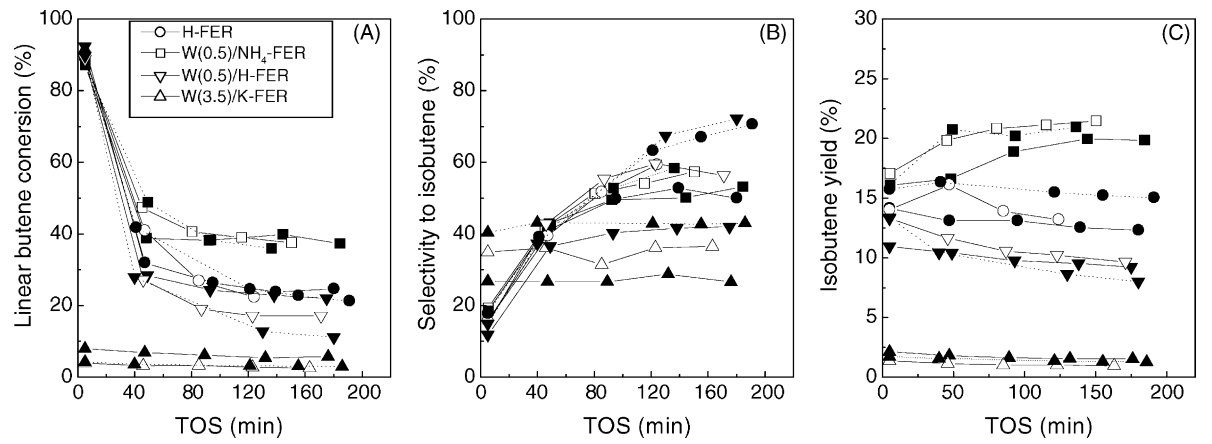

Fig. 4. (A) Linear butene conversion; (B) selectivity to isobutene; and (C) isobutene yield during the 1-butene skeletal isomerization on samples with and without tungsten, in the absence of hydrogen (filled symbol and dashed line), with pretreatment with hydrogen (open symbol and solid line) and in the presence of hydrogen during pretreatment plus reaction (filled symbol and solid line). Reaction at 300 °C, atmospheric pressure, and 0.16 atm 1-butene partial pressure.

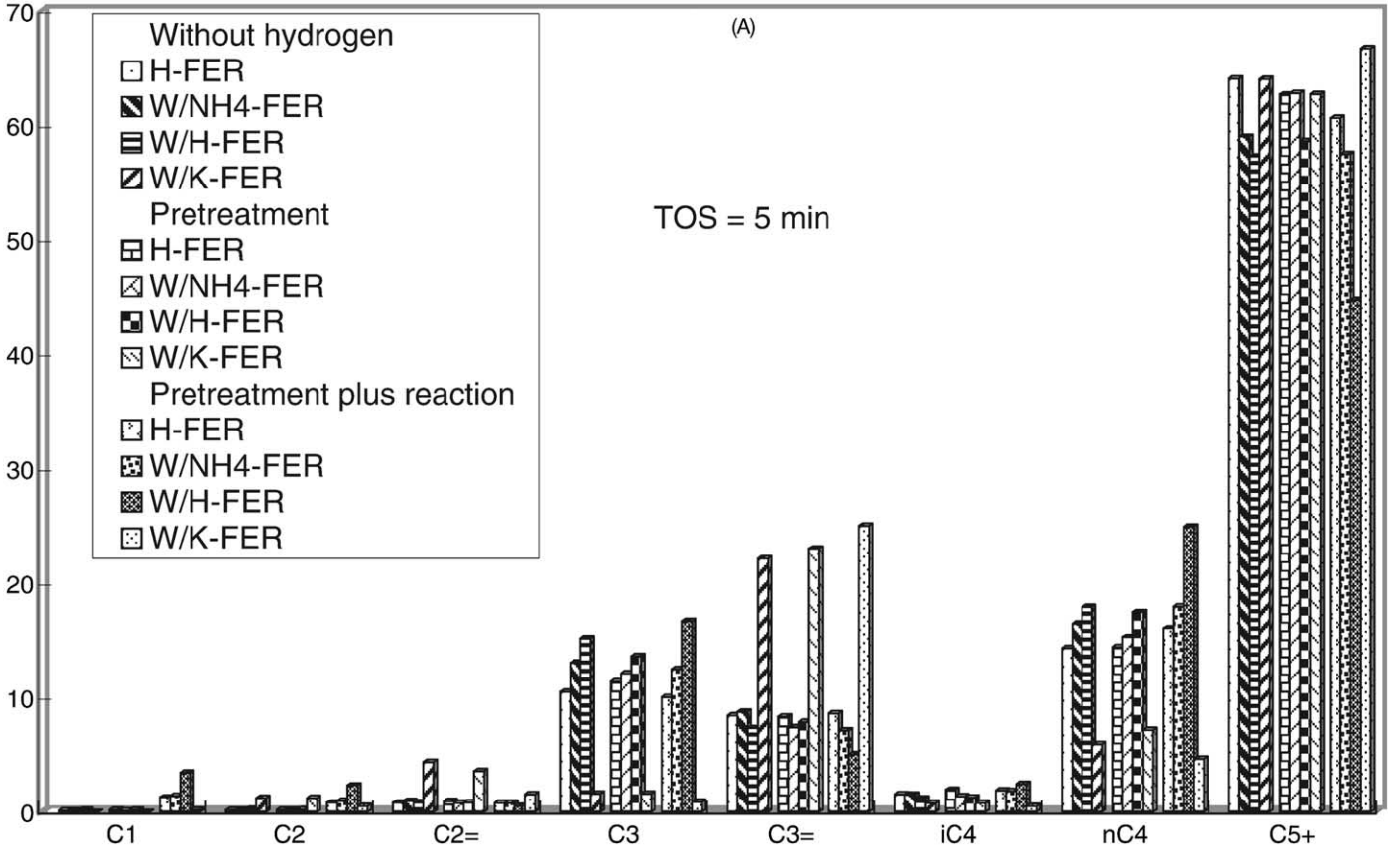

Fig. 5. By-product distributions at 5 min (A) and 140 min (B) corresponding to the 1-butene reaction on samples with and without tungsten. Reaction at 300 °C, atmospheric pressure, and 0.16 atm 1-butene partial pressure.

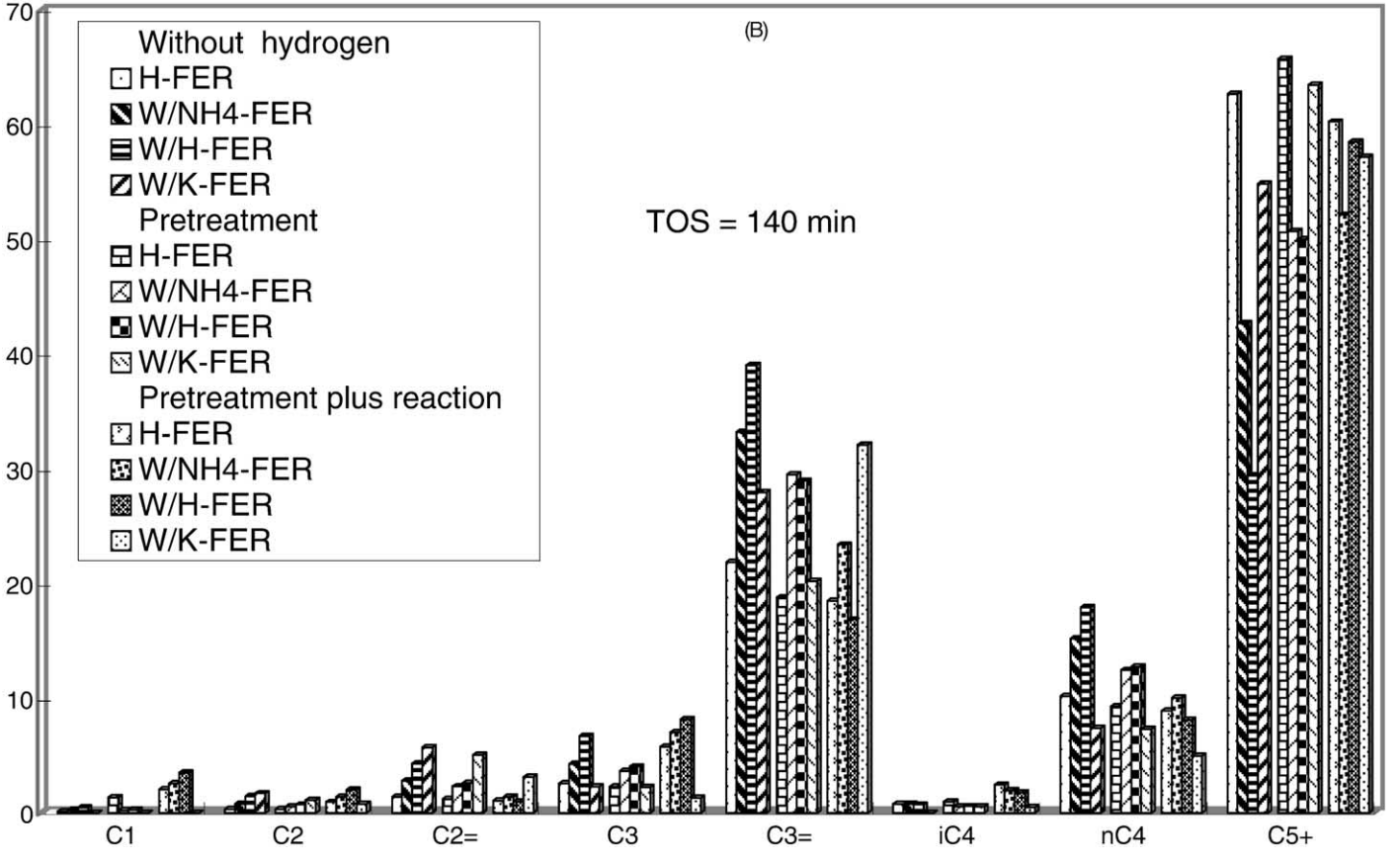

Fig. 5. (*Continued*).

observed, and the C_5^+ fraction is the most important one. H-FER, W/NH_4-FER and W/H-FER present a similar proportion of propane and butane, and a smaller amount of propene at 5 min (Fig. 5A). At long TOS (Fig. 5B) propene is the second most important fraction followed by butane and then by propane and ethene in lower proportions. Fig. 6 displays a by-product distribution for a representative sample comparing at 5 and 140 min. The most significant change occurs with propene, which increases for long TOS. This effect is more important in the absence of hydrogen. The most important fraction, the C_5^+ one, and propane decrease with TOS. This decay is lower in the presence of hydrogen. Butane decreases with TOS when hydrogen is present, the drop being higher when hydrogen is present during the reaction. At 5 min, propane is higher than propene while this ratio is inverse at long TOS. W/K-FER presents a different behavior, as shown in Figs. 5A and B. For both TOS, propene is significantly larger than propane, which is almost negligible, butane being also in low proportion.

3.5. Deactivation

Table 2 presents the amount of carbonaceous deposits formed on materials after the linear butene reaction, and the temperature of maximum of combustion peaks in the TPO profiles. Levels of carbonaceous deposits between 6.0 and 7.8% are reached on H-FER, W/NH_4-FER and W/H-FER. It agrees with results previously reported [1–3,10,14]. The deposit formed on W/K-FER is significantly lower, between 0.3 and 0.7%. Fig. 7 displays TPO profiles of characteristic samples under different operational conditions. After reaction at 300 °C, the H-FER, W/NH_4-FER and W/H-FER corresponding profiles show two well-defined combustion peaks, with a maximum at about 340–370 and 655–685 °C, respectively, and a small peak not fully resolved from the other two at about at 450–480 °C. After reaction at 450 °C, only the high-temperature combustion peak appears, without important changes in the amount of coke formed. For W/K-FER and reaction at 300 °C, the largest

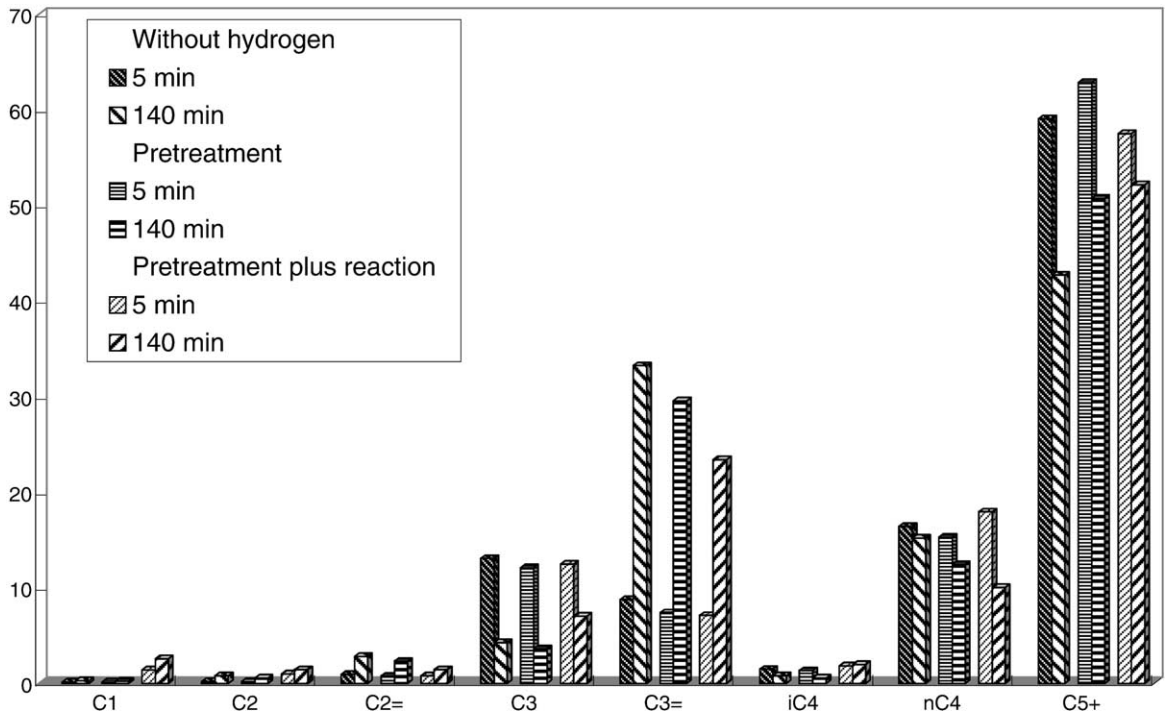

Fig. 6. Effect of TOS over by-product distribution corresponding to W/NH_4-FER, in the absence of hydrogen, with pretreatment with hydrogen, and in the presence of hydrogen during pretreatment plus reaction.

Table 2
Carbonaceous deposit characterization for H-FER, W/NH_4-FER, W/H-FER and W/K-FER samples submitted to different operational conditions and coked during 200 min in the 1-butene reaction

Sample	Operational conditions					Carbonaceous deposit			
	T_c (°C)	T (°C)	Hydrogen			Carbon content (%C)	T_m (°C)		
			Without	Pretreatment	P + R		Low	Moderate	High
H-FER	550	300	x			6.9	332	454	658
H-FER	600	300	x			7.1	389	478	683
H-FER	650	300	x			6.0	356	478	689
H-FER	700	300	x			7.2	367	467	667
H-FER	600	300		x		7.3	367	489	667
H-FER	600	300			x	7.1	378	–	678
H-FER	600	450	x			7.4	–	–	667
W(2.0)/NH_4-FER	600	300	x			7.6	349	462	677
W(1.5)/NH_4-FER	600	300	x			7.4	345	445	665
W(1.0)/NH_4-FER	600	300	x			7.6	349	441	651
W(0.5)/NH_4-FER	600	300	x			6.0	316	450	660
W(0.5)/NH_4-FER	600	300		x		6.4	331	457	651
W(0.5)/NH_4-FER	600	300			x	7.8	354	–	–
W(0.5)/NH_4-FER	600	450	x			7.2	–	–	667
W(2.0)/H-FER	600	300	x			6.8	364	457	655
W(1.5)/H-FER	600	300	x			6.0	310	480	680
W(1.0)/H-FER	600	300	x			7.0	358	474	674
W(0.5)/H-FER	600	300	x			7.7	360	472	672
W(0.5)/H-FER	600	300		x		7.5	354	480	686
W(0.5)/H-FER	600	300			x	6.6	366	–	662
W(0.5)/H-FER	600	450	x			6.6	–	–	665
W(2.5)/K-FER	600	300	x			0.4	350	–	–
W(3.0)/K-FER	600	300	x			0.3	340	–	–
W(3.5)/K-FER	600	300	x			0.4	310	–	–
W(4.0)/K-FER	600	300	x			0.4	348	–	–
W(3.5)/K-FER	600	300		x		0.5	342	–	–
W(3.5)/K-FER	600	300			x	0.6	366	–	–
W(3.5)/K-FER	600	450	x			0.7	–	–	588

T_c: calcining temperature; T: reaction temperature; T_m: temperature of the maximum of combustion peak; P + R: pretreatment plus reaction.

proportion of carbonaceous deposits corresponds to the 340–350 °C centered peak, a light shoulder appearing at high temperature for some samples. Only one combustion peak at high temperature (590 °C) appears when the reaction takes place at 450 °C, with a similar low-level of coke amount, as can be seen in Table 2.

4. Discussion

4.1. H-FER, W/NH_4-FER and W/H-FER samples

It has been shown that NH_4-FER and K-FER impregnated with tungsten have better catalytic behavior than the unpromoted materials [9]. The results reported in this paper indicate that the initial form of the ferrierite used as support for the tungsten precursors is an important parameter, which must be considered in the catalyst formulation. Tungsten loadings between 0.5 and 1.0% on NH_4-FER improve the performance as compared to the unpromoted material, while the tungsten addition on H-FER unfavors its catalytic behavior. The tungsten species reduction on NH_4-FER and H-FER starts at high temperatures, as shown in the TPR profiles. It could be associated to the presence of dispersed monomeric species, which can be present considering the tungsten precursor used and the low loadings obtained. This difficulty to reduce

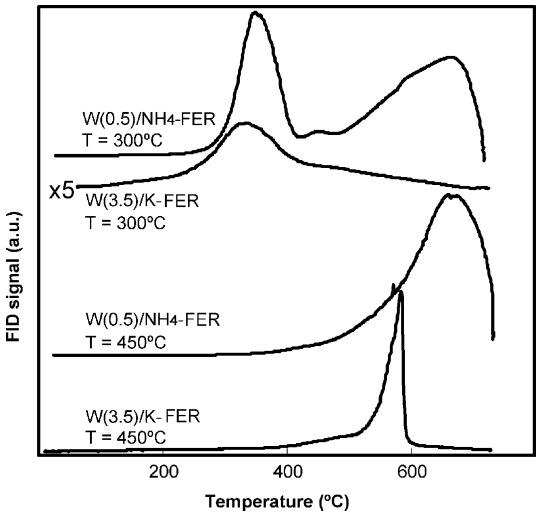

Fig. 7. TPO profiles of characteristic samples coked during 200 min at 300 or 450 °C and atmospheric pressure.

tungsten monomeric species, highly dispersed on a support such as alumina, was previously found [15]. H-FER is the form that better stabilizes the W^{6+} state, practically allowing the reduction in only one step as can be inferred from the broad reduction peak (see Fig. 1). It was explained for the W/alumina system by considering that the interaction between the oxide and the alumina prevents the WO_3 crystallite formation, which is needed in order to stabilize the lower oxidation states [16]. Furthermore, the tungsten species interaction with the H-FER surface should be higher than with the NH_4-FER one, since the reduction profile shifts towards higher temperature for the former one.

After 5 min of reaction the catalytic behavior of these samples under different operational conditions does not differ significantly one from the other, showing a high activity. Two types of acid sites were detected on these samples, with two different strengths: weak and strong, respectively [3]. At short TOS and independently of operational conditions, it can be considered that the catalytic performance of these materials is governed by the strong acid sites, which are active in oligomerization and cracking reactions responsible for the high activity with a low isobutene selectivity [4].

At long TOS, differences in the behavior appear by modifying the calcination temperature of NH_4-FER and/or by changing the reaction temperature (300 or 450 °C) on materials with and without tungsten. Working with Mo, W and Cr cations supported on silica, it was stated that acidity and cation reducibility determine both activity and selectivity during the butene skeletal isomerization reaction [17]. By considering the similar catalytic behavior at short TOS, those parameters would be not responsible for the differences observed at long TOS. Similarly, a pore blocking effect is not expected considering the tungsten precursor used. The catalytic performance of ferrierite can also be affected by the density and the space around the acid active sites [6,7], and by the shape-restriction because of coke formation inside the pores [1,6]. Previous results showed that the largest proportion of carbonaceous deposit is formed during the first 30 min under reaction conditions [18]. Consequently, it could be considered that the carbonaceous deposit influences the catalytic performance of our samples at long TOS. The low isobutene yield shown by W/H-FER at long TOS, even though this material has strong acid sites, could be understood by considering an effect of tungsten addition on the H-FER acidity. The tungsten may create new active sites by modifying the environment or by changing the site density. Then, considering also the small difference in species reducibility, the surface could be modified as coke formation takes place.

The presence of hydrogen during pretreatment or pretreatment plus reaction does not modify significantly the catalytic performance reached by the corresponding material in the absence of hydrogen. Hydrogen has little effect on the reaction. It can be related to the difficulty to reduce the tungsten species, which have no hydrogenation activity. Preliminary results using FER impregnated with other metallic species, such as nickel, having hydrogenating activity, very high conversion (almost 100%), very low isobutene yield and a significant change in the by-product distribution were obtained.

The reaction mechanism during the linear butene isomerization on ferrierite still remains under discussion. On fresh ferrierite, when the material is non-selective, it was proposed that the reaction occurs through either a bimolecular mechanism [10,19] or a monomolecular one [2,20] being the by-products formed on different active sites [20]. Evidences that a substantial amount of isobutene is formed via the non-selective bimolecular mechanism simultaneously

with the by-products were also reported [21]. On aged ferrierite, when the material became selective, it is generally accepted that the bimolecular mechanism cannot occur, and that the monomolecular one takes place instead [10,20,22]. A pseudo-monomolecular mechanism was also reported in order to explain the catalytic behavior of ferrierite [23]. In the by-product distributions shown above, the practically negligible C_1 and C_2 proportions make it possible to consider the formation of dimers and/or oligomers. The significant proportion of the C_5^+ fraction also indicates the presence of oligomeric species. At 5 min, the C_5^+ fraction is larger than propane plus propene. It can be considered that when the surface still remains "clean", when the active sites and/or their environment were not yet modified, the high reactivity of propene favors its participation in other reactions. At long TOS, the C_5^+ fraction is still lightly larger than propane plus propene. Therefore, when the largest amount of carbonaceous deposit was already formed modifying the active sites and/or their environment, the bimolecular mechanism still takes place and allows us to explain the by-product distribution. The presence of butane among the by-products can be explained considering that hydrogen transfer reactions between coke precursors and linear butene molecules take place. These reactions are considered in the mechanism of coke formation [8]. The by-product proportion decreases for all conditions at long TOS; it can be understood considering the decrease in pore volume because of the carbonaceous deposit formation, which produces catalyst deactivation [19].

The carbonaceous deposit formed on these samples after reaction at 300 °C shows two well-defined combustion peaks, the high-temperature peak being the only one present when the reaction takes place at 450 °C. FTIR characterization detects the presence of both olefinic and aromatic species in the deposit formed at 300 °C, while a mainly aromatic nature corresponds to the deposit formed at 450 °C, which need higher temperatures to burn-out. Previous results showed that the acid sites strength determines not only the amount of carbonaceous deposit but also its degree of condensation. Consequently, the presence of strong acid sites on H-FER, W/NH_4-FER and W/H-FER allows a strong adsorption of reactant molecules and/or reaction intermediates and favors the carbonaceous deposit formation. As shown in Fig. 7, the reaction temperature has also a strong influence on the type of coke. At higher reaction temperature, the amount of the aromatic coke is proportionally higher than the olefinic coke, because a higher temperature favors the aromatization of oligomers, as previously shown [11]. However, part of the aromatic coke is formed during the TPO analysis. When the temperature is increased during the TPO above the reaction temperature, several processes take place simultaneously: oxidation, cracking, and reorganization from the olefinic to the aromatic structure. This latter process generates aromatic coke on acid materials.

4.2. W/K-FER samples

K-FER is inactive in the linear butene skeletal isomerization while the addition of tungsten promotes the isobutene production [9]. Tungsten loadings between 3.5 and 4.0% lead to the best catalytic performance. The TPR characterization of WO_3 showed that reduction begins below 500 °C, displaying maxima at 656 and 763 °C, which shift to higher temperatures according to the sample size [24]. The presence of more than one peak in the reduction profiles of W/K-FER catalysts allows us consider that reduction takes place in consecutive steps, although the proportion between peaks indicates that it does not occur just by the simple sequence $W^{6+} \rightarrow W^{4+} \rightarrow W^0$. This could indicate different interactions of tungsten species on the surface. This interaction is not as strong as in the W/alumina system, where the beginning of the reduction process shifts to significantly higher temperatures [15,16]. Acidity and cation reducibility determine both activity and selectivity during the butene skeletal isomerization [17], as was above mentioned. Previous results showed that K-FER has only acid sites with weak acid strength and the presence of tungsten species on this material does not significantly modify the acid strength distribution of the unpromoted catalyst [3]. Nevertheless, the catalytic performance can be influenced not only by acidity and acid strength distribution but also by the type of acid sites [5]. Tungsten impregnation on alumina promotes the butene skeletal isomerization without modifying the acidity profile of alumina; this behavior was explained considering that Lewis acid sites are transformed into Brønsted acid sites [25]. Brønsted acidity was associated to WO_3 species or well-dispersed cations and considered

essential when the butene skeletal isomerization takes place through an alkoxide intermediate [17]. On ferrierite, the isobutene formation was related to the concentration of Brønsted acid sites, while Lewis acid sites favor butene dimerization and oligomerization [26]. W/K-FER does not reach a high activity at 5 min, showing a good stability along TOS. This behavior was associated to the absence of strong acid sites, which are related to side-reactions such as oligomerization and cracking. The acid sites that were modified and/or generated by tungsten species on K-FER have weak acid strength and are active sites, which favor the isobutene and by-product, desorption.

The presence of hydrogen during either pretreatment or pretreatment plus reaction does not modify significantly the catalytic behavior of these samples at 300 °C, the effect over by-product distribution being small. Tungsten species on these samples are also difficulty to reduce; then, no hydrogenation activity is observed, similarly as mentioned above. Nevertheless, the by-product distribution is different comparing to the ones corresponding to H-FER, W/NH_4-FER and W/H-FER. For W/K-FER, propene as second fraction following the C_5^+ one even at long TOS, and the practically negligible proportion of propane indicate a change in the material performance, which can be related to the deactivation process. The largest proportion of carbonaceous deposit corresponds to the moderate-temperature combustion peak (centered at about 340–350 °C), being associated to a coke with a higher hydrogen content [3]. The high-temperature combustion peak remains small. It can be considered that the presence of acid sites with weak strength only, unfavors the formation of carbonaceous deposit, which is more hydrogenated, and modifies the by-product distribution. When the reaction takes place at 450 °C, the amount of coke remains low and the deposit formed has a more aromatic nature although strong acid sites are not present. The strong acid sites favor a stronger adsorption of either reactants or reaction intermediates, while the weak acid sites allow the desorption of reaction products before their transformation into coke. Both weak and strong acid sites allow coke formation although the weak acid ones give a significant lower amount. Then, the strength of acid sites determines the carbonaceous deposit amount. Previous results showed a deposit with more olefinic nature when reaction takes place at low temperature while the coke formed at high temperature has mainly an aromatic character [18]. de Jong et al. [10] reported the carbonaceous deposit formed has initially an oligomeric nature, its slow aromatization then occurring. According to our results after reaction at 450 °C, the carbonaceous deposit formed on W/K-FER having only weak acid sites, also shows mainly an aromatic nature. Consequently, the nature of carbonaceous deposit is more strongly influenced by the reaction temperature than the strength of acid sites present on samples.

5. Conclusions

- NH_4-FER, H-FER and K-FER were impregnated with tungsten species. It was found that the form used as starting material is important, affecting the catalytic behavior. Tungsten loadings between 0.5 and 1.0% on NH_4-FER produce a synergetic effect over both activity and isobutene yield. Tungsten addition on H-FER worsens the unpromoted material performance. The presence of tungsten species on K-FER promotes the linear butene skeletal isomerization, with an optimum in the catalytic performance for tungsten loadings between 3.5 and 4.0%.
- The TPR characterization shows that tungsten species have the weakest interaction with the K-FER surface. The interaction on H-FER is slightly stronger than on NH_4-FER, and the reduction takes place practically in only one step.
- The higher the calcination temperature of NH_4-FER, the lower both linear butene conversion and isobutene yield.
- H-FER, W/NH_4-FER and W/H-FER, materials having both weak and strong acid sites, show similar qualitatively behaviors.
  - After 5 min of reaction and independently of operational conditions, a similar high activity with low isobutene selectivity is found. This behavior is related to the presence of strong acid sites.
  - At long TOS, the linear butene conversion at 450 °C is significantly larger than the one reached at 300 °C, while the isobutene yield remains between 12 and 18% for both reaction temperatures.
- W/K-FER samples display a different behavior.
  - At 5 min the high activity is not reached, both the linear butene conversion and isobutene yield

appearing more stable with TOS. This is associated with the absence of strong acid sites.
  - When the reaction takes place at 450 °C, the isobutene yield significantly increases, reaching a yield similar to that of the former samples.
- For all samples, the presence of hydrogen previous to and during reaction does not modify significantly the catalytic behavior, showing a small effect over the by-product distribution. By-products are formed from oligomers, being still observable at long TOS.
- The level of carbonaceous deposits formed during reaction on H-FER, W/NH_4-FER y W/H-FER was usually 6.0–7.8 wt.%, the oxidation profiles displaying two combustion peaks when the reaction took place at 300 °C, and only the high-temperature combustion peak for the reaction at 450 °C. On W/K-FER, the deposit is considerably smaller (0.3–0.7 wt.%) than in the other samples. Coke formed at 300 °C shows a well-defined combustion peak at moderate temperature, while the high-temperature combustion peak appears when the coke was formed at 450 °C. The amount of carbonaceous deposit is associated to the strength of acid sites present. Strong acid sites produce a larger deposit, which should be related to a strong adsorption of reactants and/or reaction intermediates, while weak acid sites allow product desorption rather than coke formation. The deposit nature is more strongly influenced by the temperature. The higher the reaction temperature, the more aromatic the deposit nature.

Acknowledgements

The authors are indebted to TOSOH for the provision of ferrierite samples. The financial support of CAI + D (UNL) is acknowledged. The authors wish to thank G. Brascó for his collaboration in sample preparation, and E. Grimaldi for her help in editing the English manuscript.

References

[1] W.Q. Xu, Y.G. Yin, S.L. Suib, C.L. O'Young, J. Phys. Chem. 99 (1995) 758.
[2] G. Seo, H.S. Jeong, D.L. Jang, D.L. Cho, S.B. Hong, Catal. Lett. 41 (1996) 189.
[3] Z.R. Finelli, C.A. Querini, N.S. Fígoli, R.A. Comelli, Appl. Catal. A 216 (2001) 91.
[4] Z.R. Finelli, C.A. Querini, R.A. Comelli, Catal. Lett. 78 (2002) 339.
[5] W.Q. Xu, Y.G. Yin, S.L. Suib, J.C. Edwards, C.L. O'Young, J. Phys. Chem. 99 (1995) 9443.
[6] G. Seo, N.H. Kim, Y.H. Lee, J.H. Kim, Catal. Lett. 57 (1999) 209.
[7] P. Mériaudeau, V.A. Tuan, L.N. Hung, C. Naccache, G. Szabo, J. Catal. 171 (1997) 329.
[8] S. van Donk, J.H. Bitter, K.P. de Jong, Appl. Catal. A 212 (2001) 97.
[9] Z.R. Finelli, N.S. Fígoli, R.A. Comelli, Catal. Lett. 51 (1998) 223.
[10] K.P. de Jong, H.H. Mooiweer, J.G. Buglass, P.K. Maarsen, in: C.H. Bartholomew, G.A. Fuentes (Eds.), Catalyst Deactivation 1997, Studies in Surface Science and Catalysis, vol. 111, Elsevier, Amsterdam, 1997, p. 127.
[11] R.A. Comelli, Z.R. Finelli, N.S. Fígoli, C.A. Querini, in: C.H. Bartholomew, G.A. Fuentes (Eds.), Catalyst Deactivation 1997, Studies in Surface Science and Catalysis, vol. 111, Elsevier, Amsterdam, 1997, p. 139.
[12] C.A. Querini, S.C. Fung, Appl. Catal. A 117 (1994) 53.
[13] C.L. O'Young, W.Q. Xu, M. Simon, S.L. Suib, in: J. Weitkamp, H.G. Karge, H. Pfeifer, W. Hölderich (Eds.), Zeolites and Related Microporous Materials: State of the Art 1994, Studies in Surface Science and Catalysis, vol. 84, Elservier, Amsterdam, 1994, p. 1671.
[14] M. Guisnet, P. Andy, Y. Boucheffa, N.S. Gnep, C. Travers, E. Benazzi, Catal. Lett. 50 (1988) 159.
[15] R. Thomas, E.M. van Oers, V.H.J. de Beer, J. Medema, J.A. Moulijn, J. Catal. 76 (1982) 241.
[16] I.E. Wachs, C.C. Chersich, J.H. Hardenbergh, Appl. Catal. 13 (1985) 335.
[17] N.C. Ramani, D.L. Sullivan, J.G. Ekerdt, J. Catal. 173 (1998) 105.
[18] G.N. Brascó, R.A. Comelli, Catal. Lett. 71 (2001) 111.
[19] M. Guisnet, P. Andy, N.S. Gnep, C. Travers, E. Benazzi, in: H. Chon, S.K. Ihm, Y.S. Uh (Eds.), Progress in Zeolite and Microporous Materials, Studies in Surface Science and Catalysis, vol. 105, Elsevier, Amsterdam, 1997, p. 1365.
[20] J. Houzvicka, V. Ponec, Ind. Eng. Chem. Res. 36 (1997) 1424.
[21] J. Cejka, B. Wichterlová, P. Sarv, Appl. Catal. A 179 (1999) 217.
[22] P. Mériaudeau, R. Bacaud, L. Ngoc Hung, A.T. Vu, J. Mol. Catal. A 110 (1996) L177.
[23] P. Andy, N.S. Gnep, M. Guisnet, E. Benazzi, C. Travers, J. Catal. 173 (1998) 322.
[24] D.C. Vermaire, P.C. van Berge, J. Catal. 116 (1989) 309.
[25] S.L. Soled, G.B. McVicker, L.L. Murrell, L.G. Sherman, N.C. Dispenziere, S.L. Hsu, D. Waldman, J. Catal. 111 (1988) 286.
[26] B. Wichterlová, N. Zilkova, E. Uvarova, J. Cejka, P. Sarv, C. Paganini, J.A. Lercher, Appl. Catal. A 182 (1999) 297.
[27] K.P. de Jong, W. Bosch, T.D.B. Morgan, in: A. Frennet, J.-M. Bastin (Eds.), Catalysis and Automotive Pollution Control. III. Studies in Surface Science and Catalysis, vol. 96, Elsevier, Amsterdam, 1995, p. 15.
[28] M.R. Sad, C.A. Querini, R.A. Comelli, N.S. Fígoli, J.M. Parera, Appl. Catal. A 146 (1996) 131.